# 論文 / 著書情報
# Article / Book Information

| | |
|---|---|
| 題目(和文) | 核生成界面を制御する溶液プロセス －異方成長$CeO_2$ナノワイヤー、$CeO_2$膜および$ZnO$膜の作製－ |
| Title(English) | Solution-based Process Controlling Nucleation Interfacial Behavior —Fabrication of Anisotropic $CeO_2$ Nanowires, $CeO_2$ Films and ZnO Films— |
| 著者(和文) | 久保田雄太 |
| Author(English) | Yuta Kubota |
| 出典(和文) | 学位:博士(工学),<br>学位授与機関:東京工業大学,<br>報告番号:甲第11142号,<br>授与年月日:2019年3月26日,<br>学位の種別:課程博士,<br>審査員:松下 伸広,矢野 哲司,中島 章,宮内 雅浩,生駒 俊之 |
| Citation(English) | Degree:Doctor (Engineering),<br>Conferring organization: Tokyo Institute of Technology,<br>Report number:甲第11142号,<br>Conferred date:2019/3/26,<br>Degree Type:Course doctor,<br>Examiner:,,,, |
| 学位種別(和文) | 博士論文 |
| Category(English) | Doctoral Thesis |
| 種別(和文) | 要約 |
| Type(English) | Outline |

# Solution-based Process Controlling Nucleation Interfacial Behavior —Fabrication of Anisotropic $CeO_2$ Nanowires, $CeO_2$ Films and ZnO Films—

Thesis Submitted to Tokyo Institute of Technology
By Yuta Kubota
*In Partial Fulfillment of Requirements*
*for the Degree of Doctor of Engineering*
*Main Supervisor: Prof. Nobuhiro Matsushita*
*Vice Supervisor: Prof. Tetsuji Yano*
*Department of Materials Science and Engineering*
*Japan/ March 2019*

## *Thesis Overview*

Novel solution-based processes, named as gas-liquid precipitation and gas-assisted liquid phase deposition (G-LPD), were developed in this thesis. The unique point and aims of these processes are usage of gaseous $NH_3$ generated from aqueous solution of $NH_3$ or compounds, which generated $NH_3$ by hydrolysis, and heterogeneous nucleation at the gas-liquid interface and the solid-liquid interface. $CeO_2$ nanowires having several micrometers in length were fabricated at temperature under 60 °C without any additives by the gas-liquid precipitation process. It was revealed that the mesocrystal formation at the gas-liquid interface was one of the key factors to induce the anisotropic growth. On the other hand, $CeO_2$ films and ZnO films were fabricated at 60 °C without their seed layers using readily available metal salts such as nitrates and chlorides by the G-LPD process and the modified G-LPD process using ethylene glycol as the solvents. In the G-LPD process, the pH value of the aqueous metal salts solution was an important parameter to fabricate crystalline oxide films. The fabricated ZnO films had the continuous film structure because of the adhesion of ethylene glycol to the surface of the ZnO films, and they exhibited visible light transmittance greater than 60% and the decrease in the electrical resistivity under UV-A irradiation. These solution-based processes represented a way for functional oxides to form their oriented mesocrystals depending on their surface energies and to transform into the designated shapes like wires and sheets, and to form films under mild conditions.

The thesis is composed of 6 chapters.

## *Chapter 1: Background and Objective of This Study*

Solution processes for fabricating functional oxides in the shapes of anisotropic nanoparticles, such as nanowires, nanorods and nanosheets, and films have been widely studied, since anisotropic nanoparticles have attractive unique optical, magnetic and chemical properties and films are simple to apply devices. In the case of anisotropic nanoparticles fabrication, they are normally fabricated using templates, such as surfactants, matrix and mesoporous materials with nanochannels. However, it results in requirement for a purification process, and low purity. Although there are template free approaches, they require the well understanding of intrinsic crystal plane properties of the materials and the ability of the anions in the solution to stabilize a certain crystal plane. From the point of simple view, template free approach is regard as a low environmental load process for fabricating anisotropic nanoparticles. Therefore, there is a demand to reveal a formation mechanism of anisotropic nanoparticles by the template free process, according to their surface energies of crystal planes and the stabilization of crystal planes due to anions adsorption. On the other hand, in case of films fabrication, they are fabricated by a thermal decomposition process of metal salt solutions that are spun-cast onto a substrate, or a chemical bath deposition process using their seed layers. Since these seed layers are prepared by a thermal decomposition process, the total process temperature is generally above 200 °C. In recent years, a liquid phase deposition (LPD) process using a metal fluoro complex and $H_3BO_3$ as an $F^-$ scavenger has been widely studied because it can provide oxide/hydroxide films without using seed layers at reaction temperatures below 100 °C. However, this process is only applicable to oxides whose metal ions form fluoro complexes because the oxide films are formed through a hydrolysis equilibrium reaction. Therefore, there is still a need to develop other LPD processes to fabricate oxide films using readily available metal salts such as nitrates and chlorides.

The main focuses of the thesis were as follows;

(1) To fabricate $CeO_2$ anisotropic nanoparticles without any additives by a gas-liquid precipitation process developed in the thesis.

(2) To propose formation mechanism of $CeO_2$ nanowires and nanorods in the gas-liquid precipitation process.

(3) To fabricate crystalline $CeO_2$ films without their seed layers by a gas-assisted liquid phase deposition (G-LPD) process developed in the thesis using readily available metal salts such as nitrates and chlorides.

(4) To fabricate crystalline ZnO films without their seed layers by the modified G-LPD process, and expand the applicable range of the G-LPD process.

## *Chapter 2: Novel Solution-based Processes*

The developed solution-based processes, named gas-liquid precipitation process and gas-assisted liquid phase deposition (G-LPD) process, were explained in detail in this chapter. Figure 2.1 shows a schematic image of the gas-liquid precipitation process. This process is carried out by vaporizing $NH_3$ from an $NH_3$ gas generating solution, and the generated gas reaches the surface of a starting material solution, which induces precipitation at a gas-liquid interface. In the gas-liquid precipitation process, soluble metal salts, such as nitrates and chlorides, can be used as the starting material. An aqueous $NH_3$ solution is used as the $NH_3$ gas generating solution. In the G-LPD process, aqueous solution of chemical compounds, which generated $NH_3$ by hydrolysis, are used as the $NH_3$ gas generating solution instead of the aqueous $NH_3$ solution. The aims of these processes are heterogeneous nucleation at a gas-liquid interface and a solid-liquid interface. In the gas-liquid precipitation process, the gaseous $NH_3$, which is introduced to an aqueous metal salt solution, induces oxide precipitation at the gas-liquid interface. The interface plays a role as a soft template to fabricate anisotropic nanoparticles. In the G-LPD process, a small amount of generated and introduced gaseous $NH_3$ controls the pH of the metal salt solution in a preferable pH range for the direct oxide formation. The detail explanation and calculation of the preferable pH range are described in this chapter. From these calculations, grouping of elements according to easily formed compound and reaction route in the aqueous metal salts solution at 60 °C is summarized in Table 2.1. Furthermore, experimental parameters, affected process elements, influences on products and their relationship in gas-liquid precipitation and G-LPD are summarized in Table 2.2.

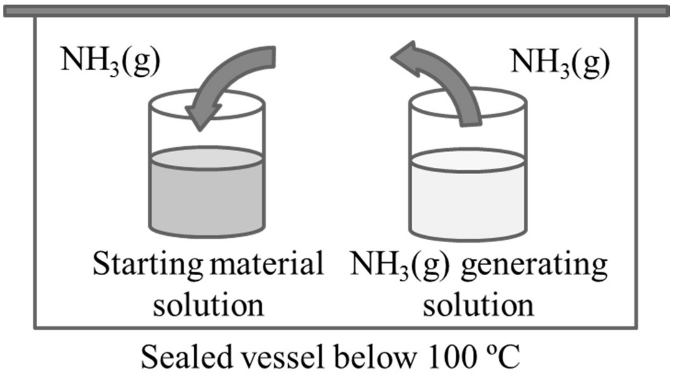

**Figure 2.1** Schematic image of the gas-liquid precipitation process.

**Table 2.1** Elements grouping according to easily formed compound and reaction route in the aqueous metal salts solution at 60 °C.

| Group | | Elements | Easily formed compound | Formation route | |
|---|---|---|---|---|---|
| 1 | | Li, Na, K, Rb, Cs, Ca, Ba, Sc | – | | – |
| 2-1 | 2-1-1 | Be, Sc, Zn, Pb, Bi | Oxide | | $M^{n+}$–$OH^-$ |
| | 2-1-2 | Mg, Y, La, Nd, Sm, Eu, Gd, Dy, Ho, Er, Tm, Yb, Lu, Cd, Al, In, | Hydroxide | | $M^{n+}$–$OH^-$ |
| 2-2 | 2-2-1 | Ce, Ti, Hf, Fe, Co, Sn | Oxide | Both of | $M^{n+}$–$OH^-$<br>and<br>$M^{n+}$–$H_2O$ |
| | 2-2-2 | Zr, Cu | Hydroxide | Both of | $M^{n+}$–$OH^-$<br>and<br>$M^{n+}$–$H_2O$ |

**Table 2.2** Experimental parameters, affected process elements, influences on products and their relationship in gas-liquid precipitation and G-LPD.

| Experimental parameters | Affected process elements | | | Influences on products |
|---|---|---|---|---|
| Process temperature | Flow speed of $NH_3$ gas | → | Reaction speed | Morphology |
| | | → | Flow volume of $NH_3$ gas | Yield, Thickness |
| | Reaction speed | | | Morphology |
| Process duration | Flow volume of $NH_3$ gas | | | Yield, Thickness |
| Concentration of starting material solution | Reaction speed | | | Morphology |
| pH of starting material solution | | | | Specie |
| | Reaction speed | | | Morphology |
| Concentration of $NH_3$ gas generating solution | Flow speed of $NH_3$ gas | → | Reaction speed | Morphology |
| | | → | Flow volume of $NH_3$ gas | Yield, Thickness |
| | Reaction speed | | | Morphology |
| Kind of $NH_3$ gas generating chemicals | Flow speed of $NH_3$ gas | → | Reaction speed | Morphology |
| | | → | Flow volume of $NH_3$ gas | Yield, Thickness |
| Volume of sealed vessel | Flow speed of $NH_3$ gas | → | Reaction speed | Morphology |
| | | → | Flow volume of $NH_3$ gas | Yield, Thickness |
| Liquid surface area | Flow speed of $NH_3$ gas | → | Reaction speed | Morphology |
| | | → | Flow volume of $NH_3$ gas | Yield, Thickness |
| Length between gas-liquid interface and substrate | Flow speed of $NH_3$ gas | → | Reaction speed | Morphology |
| | | → | Flow volume of $NH_3$ gas | Yield, Thickness |

## *Chapter 3: $CeO_2$ Nanowires and Nanorods Fabrication by Gas-liquid Precipitation Process*

$CeO_2$ nanowires with lengths of 6 μm and diameters of tens of nanometers, and nanorods with lengths of several micrometers and diameters of from tens to hundreds of nanometers were fabricated at a low process temperature of 60 °C without any additives by the gas-liquid precipitation process. Figure 3.1 shows SEM images of $CeO_2$ nanoparticles fabricated by the gas-liquid precipitation process under various conditions. According to TEM analysis, $CeO_2$ mesocrystals, which formed in an initial step of this process grew in a direction of <011> into nanowires and nanorods exposing {011} and {001} on their side walls. The formation mechanisms of nanowires and nanorods were proposed from the state of nucleation in solution, the pH at each synthesis time, and detailed TEM analysis. The proposed the formation mechanisms are shown in Figure 3.2. This solution-based process opens a way for functional oxides to form their oriented mesocrystals depending on their surface energies and to transform into the designated shapes like wires, rods and sheets.

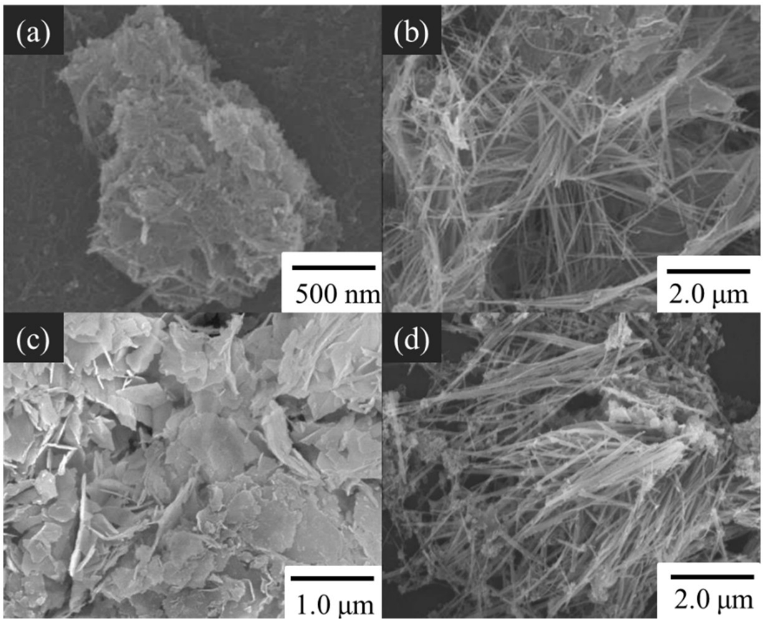

**Figure 3.1** SEM images of $CeO_2$ nanoparticles fabricated by gas-liquid precipitation under various conditions using $Ce(NO_3)_3$ solution (a) at 25 °C for 3 days, (b) at 25 °C for 10 days, (c) at 7 °C for 3 days, (d) at 60 °C for 3 days.

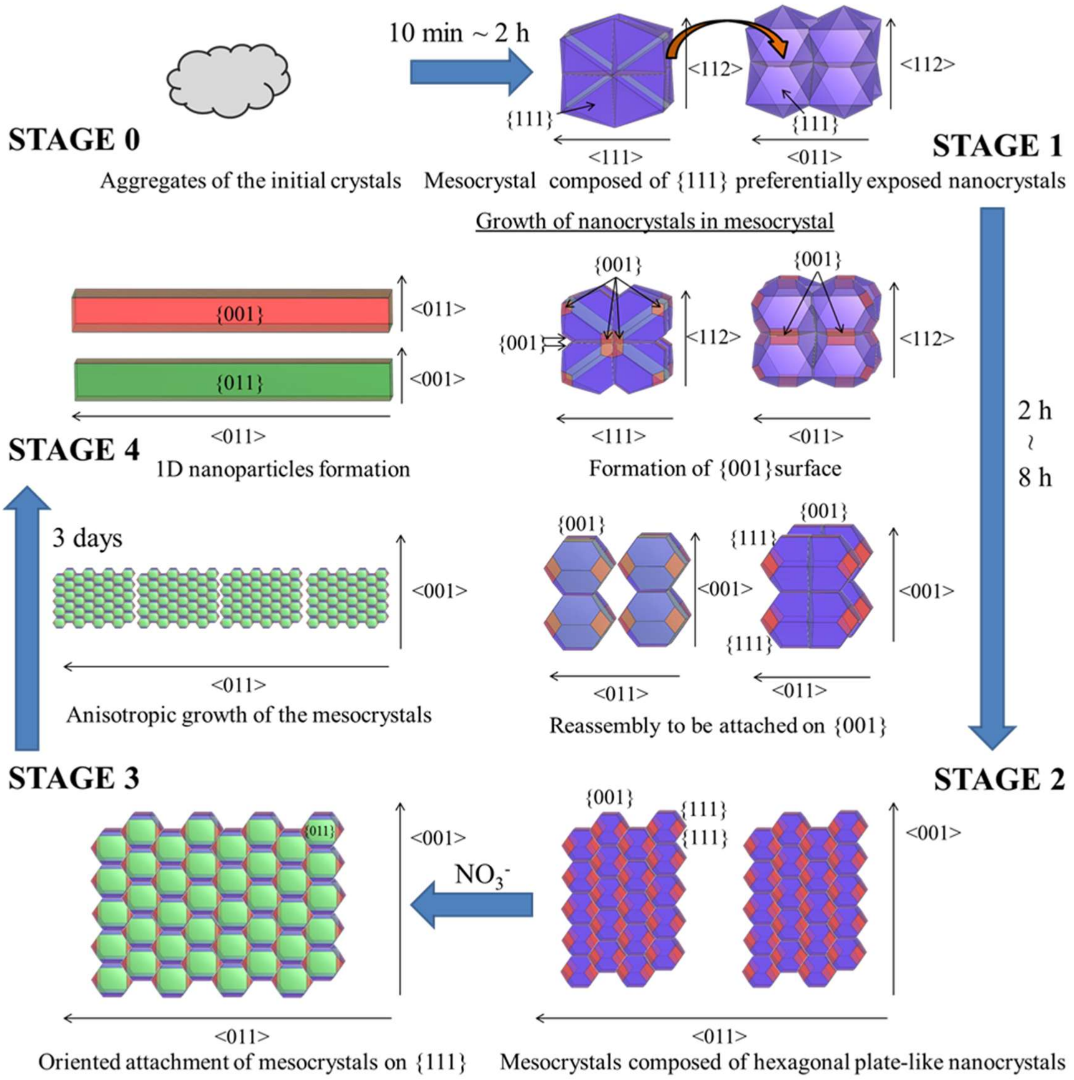

**Figure 3.2** Formation mechanisms of several micron length 1D $CeO_2$ nanoparticles by gas-liquid precipitation (from STAGE 0 to 4).

- <u>Stage 0: Formation of aggregates of the initial crystals at the gas-liquid interface</u>

  Aggregates of the $CeO_2$ initial crystals are formed at the gas-liquid interface by supply of $NH_3$ gas.

- <u>Stage 1: Formation of {111}-oriented mesocrystals due to the negative pH gradation from the gas-liquid interface to the bottom of the solution</u>

  The aggregates form for 10 min after commencement of the reaction, which have {001} and {011} surfaces, are dissolved with going down to the bottom of the container because of the negative pH gradation from the gas-liquid interface to the bottom of the solution. Crystal planes of {001} and {111} are more unstable than that of {111}. The dissolved $Ce^{4+}$ is adsorbed on the remaining $CeO_2$ {111} surface, and the {111} exposed nanocrystals are formed as a result.

- Stage 2: Growth of nanocrystals in the mesocrystals

  After the pH of the container almost becomes saturated and becomes basic, {001} and {011} are formed on the {111}-oriented $CeO_2$ nanocrystals. Since {001} is more unstable than {111}, the grown nanocrystals exposed {001} surface in the mesocrystal reassembles to be attached to each other on {001}, and then mesocrystals composed of hexagonal plate-like nanocrystals are formed.

- Stage 3: Stabilization of {001} due to $NO_3^-$ adsorption and oriented attachment of the mesocrystals on {111}

  Since the {001} surface has a strong polarity, $NO_3^-$ ions are attracted to the {001} surface, and they work as capping agents. Therefore, the oriented attachment on {001} is stopped, and the oriented attachment of mesocrystals on {111} proceeds again.

- Stage 4: Formation of $CeO_2$ 1D nanoparticles through anisotropic growth of the mesocrystals

  Proceeding the oriented attachment on {111}, $CeO_2$ 1D nanoparticles, which grow in the <011> direction, are formed as a result. The $CeO_2$ 1D nanoparticles are formed through anisotropic growth of the mesocrystals.

Publication relating this chapter

[1] Yuta Kubota, Tetsuo Kishi, Tetsuji Yano and Nobuhiro Matsushita, Anisotropic growth of gas-liquid precipitated ceria mesocrystals to wires several micrometers in length, *RSC Advances*, 2018, **8**, 24370–24375, doi: 10.1039/c8ra05362f.

## ***Chapter 4: $CeO_2$ Film Fabrication by G-LPD Process***

Crystalline $CeO_2$ films were fabricated on the plastic PES substrates and metal Ni substrates without their seed layers at a low process temperature of 60 °C by the G-LPD process using readily available metal salts such as nitrates and chlorides. Two important features of G-LPD were identified. One was controlling the pH of the aqueous metal salts solution in the range calculated in ***Chapter 2***. The other was slightly increasing the hydroxide ion concentration to facilitate oxide deposition through the heterogeneous nucleation at the solid–liquid interface. Adjusting the initial pH of aqueous the Ce salts solution to the preferable pH range, crystalline $CeO_2$ films were fabricated from not only the $Ce(NO_3)_3$ but also the $CeCl_3$ solution. Therefore, it was assumed that the kind of anions did not have critical effect on the film formation. Other oxide films, which elements belong to the group 2-2-1 (see Table 2.1), also would be formed by G-LPD with the initial pH adjustment in the preferable range. The G-LPD process represents a way to form films of functional oxides under mild conditions.

Publication relating this chapter

[1] Yuta Kubota, Tetsuo Kishi, Tetsuji Yano and Nobuhiro Matsushita, Gas-assisted liquid phase deposition of crystalline ceria films, *Surface and Coatings Technology*, 2019, **361**, 263–269, doi: 10.1016/j.surfcoat.2019.01.017.

## ***Chapter 5: ZnO Film Fabrication by G-LPD Process Using Ethylene Glycol***

Crystalline ZnO films were fabricated on the PES substrate by the modified G-LPD process using ethylene glycol (EG) as solvents. The PES substrates (2.0 cm × 3.0 cm) were adhered to the inside wall of the beaker with 2/3 of their length in the $Zn(NO_3)_2$/EG solution by using polyimide tape to cover the top of the substrate with 1/6 of their length. The fabricated ZnO films on the PES substrate near the gas-liquid interface had continuous film structure because of the adhesion of EG to the crystals, and they exhibited visible light transmittance greater than 60% and the decrease in the resistivity under UV-A irradiation. Figure 5.1 shows surface SEM images of the PES substrate that was on the wall of the beaker at different distances (*d*) from the bottom of the PES substrate. Although the pH value of the aqueous $Zn(NO_3)_3$ solution was adjusted and controlled in the preferable pH range, the ZnO formation reaction at the gas-liquid interface occurred preferentially and the heterogeneous nucleation and crystal growth at the solid-liquid interface were strongly suppressed. Therefore, the usage of EG had an effect on suppressing the drastic increase in $OH^-$ concentration of the Zn salts solution at the gas-liquid interface, where the heterogeneous nucleation was conducted by dissolving gaseous $NH_3$. The modified G-LPD process enables the fabrication of oxide films, which elements belong to the group 2-1-1 (see Table 2.1), with low environmental load using a chemical reaction that occurs at the solid-liquid interface.

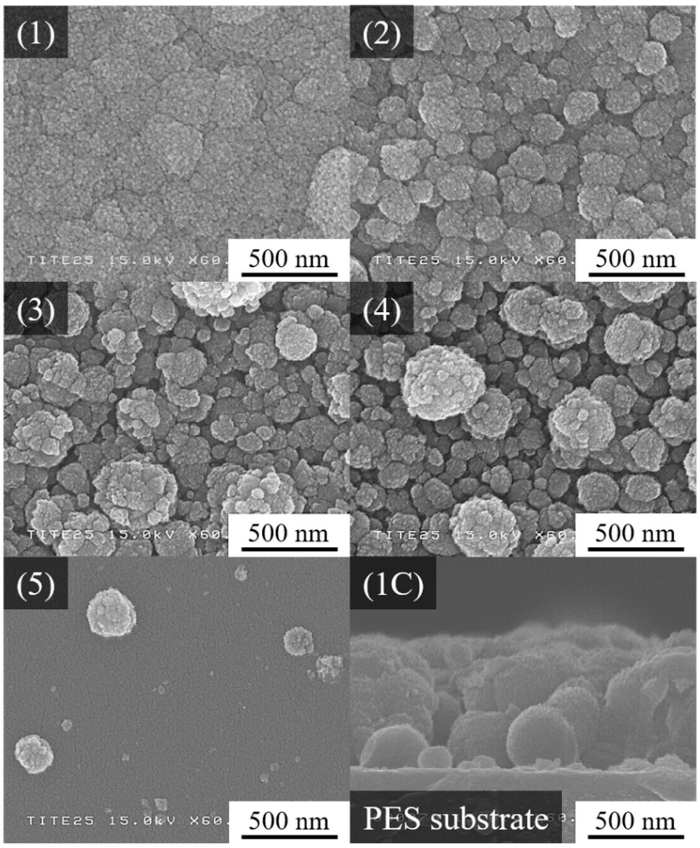

**Figure 5.1** Surface SEM images of the PES substrate that was on the wall of the beaker at different distances (*d*) from the bottom of the PES substrate: (1) $1.5 \leq d < 2.0$ cm, (2) $1.0 \leq d < 1.5$ cm, (3) $0.5 \leq d < 1.0$ cm and (4) $0 \leq d < 0.5$ cm. Surface SEM image of a PES substrate that was on the bottom of the beaker (5). Cross-sectional SEM image (1C) from section(1).

Publication relating this chapter

[1] Yuta Kubota, Tetsuo Kishi, Tetsuji Yano and Nobuhiro Matsushita, One Step Fabrication of ZnO Fims Using a Modified Gas-assisted Liquid Phase Deposition Process, *Chemistry Letters*, Advance Publication on the web January 26, 2019, doi:10.1246/cl.180975.

## ***Chapter 6: General Conclusions***

In the thesis, $CeO_2$ nanowires/nanorods, $CeO_2$ films and ZnO films were fabricated by the developed solution-based processes, named as gas-liquid precipitation and gas-assisted liquid phase deposition (G-LPD). These developed processes can fabricate functional oxides in the shapes of anisotropic nanoparticles and films at a low process temperature of ~60 °C without any additives and their seed layers. Therefore, these solution-based processes controlling nucleation interfacial behavior can be regarded as a low environmental load processes. I consider that these processes represent a way for functional oxides to form their oriented mesocrystals depending on their surface energies and to transform into the designated shapes like wires and sheets, and to form films under mild conditions.